EC Accepts, published online ahead of print on 17 November 2006
Eukaryotic Cell doi:10.1128/EC.00318-06

Vesicular polysaccharide export in *Cryptococcus neoformans* is an eukaryotic solution to the problem of fungal trans-cell wall transport[ϕ]

Marcio L. Rodrigues[1], Leonardo Nimrichter[1], Débora L. Oliveira[1], Susana Frases[2], Kildare Miranda[3], Oscar Zaragoza[2‖], Mauricio Alvarez[2], Antonio Nakouzi[2], Marta Feldmesser[2,3] and Arturo Casadevall[2,3,*].

[1]Laboratório de Estudos Integrados em Bioquímica Microbiana, Instituto de Microbiologia Professor Paulo de Góes, Universidade Federal do Rio de Janeiro, 21941590, Brazil; [2]Department of Microbiology and Immunology and the [3]Division of Infectious Diseases of the Department of Medicine, Albert Einstein College of Medicine, 1300 Morris Park Ave, Bronx, NY USA 10461; [3]Laboratório de Ultraestrutura Celular Hertha Meyer, Instituto de Biofísica Carlos Chagas Filho, Universidade Federal do Rio de Janeiro, 21941590, Brazil.

[‖]Present address: Servicio de Micología, Centro Nacional de Microbiología, Instituto de Salud Carlos III, Ctra Majadahonda-Pozuelo km 2, 28220 Majadahonda, Madrid, Spain.

*Corresponding author. Mailing address: Department of Microbiology and Immunology, Albert Einstein College of Medicine, 1300 Morris Park Avenue, Bronx, NY 10461. Phone: (718) 430-2215. Fax: (718) 430-8968. E-mail: casadeva@aecom.yu.edu.

[ϕ]MLR, LN and DLO contributed equally to this work.

Abstract

The mechanisms by which macromolecules are transported through the cell wall of fungi are not known. A central question in the biology of *Cryptococcus neoformans*, the causative agent of cryptococcosis, is the mechanism by which capsular polysaccharide synthesized inside the cell is exported to the extracellular environment for capsule assembly and release. We demonstrate that *C. neoformans* produces extracellular vesicles during in vitro growth and animal infection. Vesicular compartments, which are transferred to the extracellular space by cell wall passage, contain glucuronoxylomannan (GXM), a component of the cryptococcal capsule, and key lipids, such as glucosylceramide and sterols. A correlation between GXM-containing vesicles and capsule expression was observed. The results imply a novel mechanism for the release of the major virulence factor of *C. neoformans*, whereby polysaccharide packaged in lipid vesicles crosses the cell wall and the capsule network to reach the extracellular environment.

Introduction

Cryptococcus neoformans is a yeast-like pathogenic fungus that is the etiologic agent of human cryptococcosis. Infection is usually asymptomatic and restricted to the lung in immunocompetent individuals, but fungal cells can disseminate to other organs and cause cryptococcal meningoencephalitis, a common syndrome in immunosuppressed patients (29, 39). Significant progress in our understanding of how *C. neoformans* causes disease was made in the last decade, but many aspects of cryptococcal pathogenesis remain poorly understood.

C. neoformans represents a unique model in cell biology studies because it is the only eukaryotic pathogen with a polysaccharide capsule, a structure that is essential for virulence (4, 19). The major capsular polysaccharide, glucuronoxylomannan (GXM), has an average mass ranging from 1.7 to 7 x 10^6 daltons (22) and is released extracellularly during infection, inducing a number of deleterious effects to the host (39). GXM also represents a potential vaccine component and is the target of therapeutic antibodies that are currently in clinical trial (3, 8, 20, 27).

The fungal cell wall is a compact, albeit dynamic, structure that plays important roles in several biological processes determining cell shape, morphogenesis, reproduction, cell-cell and cell-matrix interaction, osmotic and physical protection (25). Although the relevance of the cell wall to fungal physiology and pathogenesis is clear, the mechanisms by which large molecules (molecular weight > 1 million) cross this rigid structure to reach the extracellular environment are largely unknown. In *C. neoformans*, it has been suggested that capsule components containing epitopes recognized by a monoclonal antibody (mAb) to GXM are synthesized intracellularly and exported through the cell wall, possibly inside membrane vesicles (11). These results were validated in a recent study using a secretion mutant of *C. neoformans*, in which post-

Golgi secretory vesicles containing GXM were accumulated in the plasma membrane region (40). Based on these observations one could imagine that surface components of *C. neoformans,* including the capsule, are synthesized in the cytoplasm and exported to the exterior of the cell in secretory vesicles that traverse the cell wall. Indeed, *C. neoformans* does produces glucosylceramide (GlcCer)-containing vesicles that are transferred to the cell wall (1, 25, 30). Since *C. neoformans* efficiently releases exocellular capsular material, we hypothesized the existence of extracellular secreted vesicles containing GlcCer and capsule components.

In the present work, we describe for the first time that a fungal cell can produce extracellular vesicles that are secreted across the cell wall. Supernatants of *C. neoformans* cultures contained vesicles with bilayered membranes. Lipid analysis revealed that key fungal lipids, such as glucosylceramide, ergosterol and a novel sterol, are present in these membranes. By different approaches, we demonstrated that GXM is packaged inside the vesicles, which cross the cell wall and the capsule network to reach the extracellular environment. A correlation between capsule growth and detection of vesicle-associated GXM was observed, suggesting that *C. neoformans* can release the polysaccharide from the vesicles and incorporate it into the cell surface. Accordingly, acapsular cells used vesicle-associated GXM to become encapsulated. GXM-containing vesicles were produced during macrophage infection, suggesting a role in pathogenesis. These findings illustrate a new phenomenon in fungi with potential relevance for such diverse areas as capsule assembly and pathogenesis and reveals new insights on how secreted molecules reach the extracellular environment.

Materials and Methods

Culture conditions. The cryptococcal isolates used in this study comprised strains ATCC 24067 (serotype D, American Type Culture Collection), H99 (serotype A, clinical isolate), HEC3393 (serotype A, clinical isolate), and Cap67 (acapsular mutant). In the different analyses performed, similar data were obtained with encapsulated strains. Except for the presence of GXM, results in assays using acapsular cells also followed the same profile obtained with HEC3393, H99 and 24067 cells. For vesicle purification, *C. neoformans* cells were inoculated into 1000 ml Erlenmeyer flasks containing 400 ml of a minimal medium composed of dextrose (15 mM), $MgSO_4$ (10 mM), KH_2PO_4 (29.4 mM), glycine (13 mM), and thiamine-HCl (3 µM). Fungal cells were cultivated for three days at 30°C, with shaking. The viability of *C. neoformans* cells after this period of cultivation was analyzed by propidium iodide (PI) staining.

Isolation of vesicles. Fungal cells were separated from culture supernatants by centrifugation at 4,000 *g* for 15 min at 4°C. The supernatants were collected and again centrifuged at 15,000 *g* (4°C), to remove smaller debris. The pellets were discarded and the resulting supernatant was concentrated by approximately 20-fold using an Amicon ultrafiltration system (cutoff = 100 kDa). To ensure the removal of cells and cellular debris, the concentrated culture fluid was again centrifuged as described above and the resulting supernatant was then centrifuged at 100,000 *g* for 1 h at 4°C. The supernatants were then discarded and pellets were washed by five sequential resuspension and centrifugation steps, each consisting of 100,000 *g* for 1 h at 4°C with 0.1M tris buffered saline (TBS). The pellets were then resuspended in fixative solution for electron

microscopy analysis. Alternatively, 100,000 *g* pellets were fractionated by affinity chromatography and sucrose density centrifugation or extracted with organic solvents, as detailed below. The number of vesicles was determined by flow cytometry for further analyses of GXM content and distribution.

Transmission electron microscopy (TEM). TEM was used to visualize vesicles isolated from supernatants and those that were cell-associated, *in vitro* and *in vivo*. Pellets obtained after washing and centrifugation at 100,000 *g* were fixed in 2% glutaraldehyde in 0.1 M cacodylate at room temperature for 2 h, and then incubated overnight in 4% formaldehyde, 1% glutaraldehyde, and 0.1% PBS. The samples were incubated for 90 min in 2% osmium, serially dehydrated in ethanol, and embedded in Spurrs epoxy resin. Thin sections were obtained on a Reichart Ultracut UCT and stained with 0.5% uranyl acetate and 0.5% lead citrate. Samples were observed in a JEOL 1200EX transmission electron microscope operating at 80 kV. For immunogold labeling with antibodies to GXM, the vesicles were fixed in 0.1M sodium cacodylate buffer (pH 7.2) containing 4% paraformaldehyde, 0.2% glutaraldehyde and 1% picric acid, infiltrated in 25% polyvinylpyrrolidone and 2.1 M sucrose and rapidly frozen by immersion in liquid nitrogen. Cryosections were obtained in a temperature range of –70 to –90^{0}C using a cryo-ultramicrotome (Ultracut Reichert). After blocking in PBS-BSA and 50 mM NH_4Cl, the cryosections were incubated overnight in the presence of a mouse monoclonal antibody to GXM (mAb 18B7, 1 μg/ml). The antibody is a mouse IgG1 with high affinity for GXM of different cryptococcal serotypes and has been extensively characterized previously (3). After incubation with 15 nm (particle size) immunogold-labeled anti-mouse IgG, specimens were observed in a JEOL 1200EX transmission electron microscope operating at 80 kV.

For detection of cryptococcal vesicles *in vivo*, murine infection, lung tissue preparation for transmission electron microscopy and acid phosphatase cytochemistry were done as described (10, 12). Briefly, anesthetized C57BL/6 mice (National Cancer Institute, Bethesda, MD) were infected intratracheally via a midline neck incision with 10^4 or 10^6 organisms of *C. neoformans* ATCC strain 24067 and then sacrificed 2 h, 48 h or 7 d after infection. Acid phosphatase cytochemistry was done using cytidine monophosphate (Sigma, Richmond, CA) (26), with tissue from uninfected mice and infected tissue that was not incubated in substrate serving as controls. The analysis of vesicle production in vitro was performed using strain Cap67, as previously described (30). Human antibodies to GlcCer were used for lipid detection at the cell wall, following previously described experimental conditions (30).

Removal of non-vesicular GXM from 100,000 *g* pellets. To remove extravesicular GXM and putative aggregates from vesicle preparations, 100,000 *g* pellets were purified by passage through a column packed with an antibody-bound resin. MAb 18B7 was coupled to cyanogen bromide-activated Sepharose, according to the manufacturer's protocols (Sigma, Richmond, CA). Briefly, 1 g of the resin was suspended in 1 mM HCl, washed and resuspended in carbonate buffer, pH 8.0. MAb 18B7 was dissolved in 5 ml of the same buffer, at 1 mg/ml, and incubated overnight with the resin. At this pH, mAb 18B7 retained its biological properties, such as antigen binding and integrity of chains (not shown). Coupling efficiency was ~90%, as confirmed by spectrophotometric determinations at 280 nm. After washing with carbonate buffer and blocking with 0.2M glycine, the resin was sequentially washed with 0.1 M acetate (pH 4.0) and Tris (pH 8.0) buffers, for final resuspension in PBS. Each vesicle suspension (500 μl) was mixed with the antibody-containing resin (100 μl) and incubated for 1 h (37°C) under shaking. The unbound

fraction was recovered by centrifugation. This process was repeated three times and GXM content in different fractions was analyzed by capture ELISA, as described below.

Sucrose gradient. Sucrose density centrifugation was performed as described by Gutwein et al. (15). The vesicle suspension (0.5 ml) obtained after ultracentrifugation and purification with the antibody-coupled resin was mixed with an equivalent volume of 85% sucrose (w/v in TBS), generating a final concentration of 42.5% sucrose. This suspension was transferred to an ultracentrifuge tube and a step gradient was prepared by overlaying the original suspension with 35% sucrose, followed by a final layer of 5% sucrose in TBS. The gradient was centrifuged for 18 h at 200,000 *g* and fractions of 0.25 ml were collected from the top to the bottom of the gradient. Fractions were then extensively dialyzed against TBS, dried under vacuum centrifugation and suspended in 100 μl of absolute methanol, resulting in the immediate formation of a precipitate. The solution was then extracted with 200 μl of chloroform for 1 h at 25^{o}C. The organic fraction was recovered by centrifugation and analyzed by different methods for lipid identification. The residual material that was not soluble in the chloroform-methanol mixture was then dried under a nitrogen stream, resuspended in TBS and assayed for the presence of GXM, as described later in this section.

Lipid analysis. Pellets obtained from centrifugation of cell supernatants at 100,000 *g* were first suspended in methanol and then two volumes of chloroform were added. The mixture was vigorously vortexed and centrifuged to discard precipitates, dried by vacuum centrifugation and partitioned according to Folch et al. (13). The lower phase, containing neutral lipids, was recovered for analysis by high performance thin layer chromatography (HPTLC). For sterol

analysis, the lipid extract was loaded into HPTLC silica plates (Si 60F254s, LiChrospher, Germany) and separated using a solvent system containing hexane:ether:acetic acid (80:40:2, v/v/v) solvent. The plate was sprayed with a solution of 50 mg ferric chloride ($FeCl_3$) in a mixture of 90 ml water, 5 ml acetic acid and 5 ml sulfuric acid. After heating at 100°C for 3-5 min, the sterol spots were identified by the appearance of a red-violet color. The presence of GlcCer was evaluated by separating lipids in the Folch's lower phase by HPTLC using chloroform/methanol/water (65:25:4, v/v/v). Monohexosylceramides were visualized after spraying the plates with the orcinol-sulfuric reagent followed by heating at 150°C (1).

The lower phase obtained after Folch's partition was also analyzed by electrospray ionization-mass spectrometry (ESI-MS) using a Finnigan LCQ-Duo ion trap instrument (Thermo Electron, San Jose, CA). Samples were diluted in chloroform-methanol (1:1, vol/vol), containing 10 mM lithium iodide, and introduced into ESI-MS at 10 µl/min flow rate, with the assistance of an infusion micropump (Harvard Apparatus, Cambridge, MA). Analyses were carried out in the positive (ESI+) mode. The source and capillary voltages were 4.5 kV and 3 V, respectively. The capillary temperature was kept at 200°C. Spectra were collected at a 300- to 800-*m*/*z* range. Source-induced dissociation was obtained at 25 V. Ion trap collision-induced dissociation (ESI-MS/MS) experiments were carried out at 20 to 60% (1 to 3 eV) normalized relative collision energy. All spectra were processed using the Xcalibur software (Thermo Electron).

Lipids in fractions from the sucrose gradient were analyzed by high performance liquid chromatography (HPLC) in a Waters 600 liquid chromatograph (New York, NY), using an Alltech C_{18} column (Deerfield, IL) (250 x 4.6 mm dimensions, 5 µm particle size). A mixture of chloroform and methanol (9:1, v/v) was used as the mobile phase and lipid components were

detected by absorbance at 280 nm in a Waters 486 detector. The profile of elution of lipids from sucrose gradient fractions was compared with a standard of purified cryptococcal GlcCer (30).

Radioactive labeling of vesicles. *C. neoformans* (strain 24067) was grown in the presence of L-[^{3}H]serine (20 Ci/mmol) (American Radiolabeled Chemicals, Inc., St. Louis, MO) and [9,10-^{3}H]palmitic acid (50 Ci/ mmol) (DuPont NEN, Boston, MA). These ceramide precursors were added to the culture medium described in "Culture conditions" to generate final amounts of radioactivity corresponding to 2.0 μCi/ml ([^{3}H]serine) and 1.0 μCi/ml ([^{3}H]palmitic acid). The culture was incubated for 3 days at 30ºC, and then fungal cells were removed by centrifugation. Vesicles were obtained as described above and suspended in methanol (100 μl). Chloroform (200 μl) was added and the mixture was centrifuged to discard precipitates. The lipid extract was loaded into HPTLC plates and separated using chloroform/methanol/water (65:25:4, v/v/v) as the solvent system. Molecules with migration rates corresponding to GlcCer, identified by comparison with an iodine-stained standard of glucocerebroside (Avanti Polar Lipids, Alabaster, AL), were scraped off the plate, suspended in scintillation liquid and counted for radioactivity. Negative controls included 100,000 *g* pellets from sterile medium containing the radioactive precursors and vesicle-depleted culture supernatants.

Fungal killing and lipid detection. To evaluate whether cryptococcal vesicles were physiologically released or were simply an artifact of dead cells, we evaluated the presence of lipid markers in 100,000 *g* pellets of living and dead cells. Cryptococci were treated with 10 mM sodium azide in PBS for 60 min at 25^{o}C or, alternatively, suspended in PBS and heated at 50^{o}C for the same period. Control cells (viable) were suspended in PBS and incubated at 25^{o}C for 60

min. Cell viability was evaluated by inoculating control or treated yeasts onto Sabouraud dextrose agar (SDA) and counting of colony forming units (CFU). After incubation in the conditions described above, yeasts were removed as described previously in this section and the supernatants ultracentrifuged at 100,000 *g*. The resulting pellets were extracted with mixtures of chloroform-methanol 2:1 (for GlcCer analysis) or 9:1 (for sterol analysis). Extracts were analyzed by HPTLC following the conditions described in "Lipid analysis".

Serological assays for GXM detection. The profiles of GXM distribution in the fractions obtained after sucrose density centrifugation were analyzed by using a capture enzyme-linked immunosorbent assay (ELISA) (2). Briefly, each well of a 96-well polystyrene plate was coated with a goat anti-mouse IgM. After removal of unbound antibodies, a solution of mAb 12A1, an IgM mAb with specificity for GXM, was added to the plate, and this step was followed by blocking with 1% bovine serum albumin. The ELISA was used to analyze vesicles after treatment with methanol and chloroform, as described in "Lipid analysis". Purified GXM was used as a positive control. The samples were incubated in the plate overnight at 4°C. The plates were then washed five times with a solution of TBS supplemented with 0.1% Tween 20, followed by incubation with mAb 18B7 for 1 h. The plate was again washed and incubated with an alkaline phosphatase-conjugated goat anti-mouse IgG1 for 1 h. Reactions were developed after the addition of *p*-nitrophenyl phosphate disodium hexahydrate, followed by reading at 405 nm with a Multiscan MS (Labsystem, Helsinki, Finland). Antibodies in this assay were all used at a concentration of 1 μg/ml.

Extracellular formation of GXM-containing vesicles. To explore the possibility that cryptococcal vesicles were formed as a result of random aggregation of lipids and GXM in the extracellular environment, minimal medium was supplemented with GXM (15 μg/ml) and inoculated with Cap67 cells, which are known to produce vesicles (Figures 1, 3 and 5). After growth for 72 h at 30°C, supernatants were collected and evaluated for GXM-containing vesicles. Alternatively, acapsular cells were grown in the absence of GXM and the polysaccharide was added to culture supernatants at the same concentration after removal of yeast cells, followed by incubation for 1 h at 30°C. GXM-containing supernatants were centrifuged at 100,000 *g* and the pellets purified in Sepharose-bound mAb 18B7. GXM in supernatants and 100,000 *g* pellets were then quantified by capture ELISA. The negative control consisted of GXM determinations in regular Cap67 cultures.

Capsule induction. Capsule expression in *C. neoformans* was induced as described (42). Briefly, *C. neoformans* was inoculated in Sabouraud broth diluted 10 times in MOPS 50 mM, pH 7.3. After incubation for 6 or 24 h at 37° with shaking, the cells were recovered by centrifugation for 10 min at 2,000 *g* and fixed in 2% paraformaldehyde in TBS. The fixative agent was removed by washing with PBS and, after staining with India ink, capsule expression was analyzed microscopically. Capsule sizes, defined as the distances between the cell wall and the outer border of the capsule, were determined by using the ImageJ Software, elaborated and provided by National Institutes of Health (NIH, http://rsb.info.nih.gov/ij/). All experiments were performed in triplicate sets and the results analyzed by using Student's *t* test. Supernatant-associated vesicles produced as described above were then purified by affinity chromatography and different centrifugation steps, as described previously in this section. GXM concentration in

100,000 *g* fractions in the different conditions of capsule induction was normalized to the number of cells in the culture after each condition of stimulation, as measured in a Neubauer chamber.

GXM binding by acapsular cells. Acapsular *C. neoformans* cells (strain cap 67, 10^6 cells) were suspended in 100 µl of a purified vesicular suspension with a GXM concentration corresponding to 10 µg/ml. The suspension was incubated for 12 h at 25°C and extensively washed with PBS, followed by fixation with 4% paraformaldehyde. The cells were further blocked for 1 h in PBS-BSA and incubated with mAb 18B7 (1 µg / ml) for 1 h at room temperature, followed by a fluorescein isothiocyanate (FITC) labeled goat anti-mouse IgG (Fc specific) antibody (Sigma). Yeast cells were finally observed with an Axioplan 2 (Zeiss, Germany) fluorescence microscope. Images were acquired using a Color View SX digital camera and processed with the software system analySIS (Soft Image System). In control systems, mAb 18B7 was replaced by irrelevant antibodies. In addition, vesicle preparations were simply removed from the experimental system (negative control) or replaced by soluble, non-vesicular GXM (positive control), purified as described elsewhere (6).

Production of GXM-containing vesicles during the *in vitro* infection of macrophages with *C. neoformans*. The ability of cryptococci to produce GXM-containing vesicles during the infection of host cells was evaluated using the J774.16 cell line, which has been extensively used to study *C. neoformans*-mouse macrophage interactions. Macrophage-like cells were cultured in DMEM supplemented with 10% FCS, 10% NCTC-109, and 1% nonessential amino acids, at 37°C in a 5% CO_2 atmosphere. Cultures were also supplemented with 100 U/ml IFN-γ and 1

μg/ml LPS. The cells were grown to confluence in 75 cm^2 flasks and then infected with *C. neoformans* (10 yeast per host cell) in the presence of 10 μg/ml of mAb 18B7, which binds to the capsular polysaccharide and is opsonic (3). After 1 h of incubation at 37^0C, free *C. neoformans* cells were removed by washing. Based on the observation that J774.16 cells lyse after hosting intracellular replication of cryptococci (38), washed infected cells were incubated for 18 h at 37^0C. Host cell lysis and cryptococcal intracellular replication were observed microscopically. Fluids from infected cultures were then analyzed for vesicles as described above.

Results

Production of extracellular vesicles by *C. neoformans*. Several lines of evidence suggested us that secretion of macromolecules by fungi could rely on vesicular transport (11, 14, 30-32, 35, 36, 40) and consequently, we designed experiments to search for vesicles in fungal cells and culture supernatants. In acapsular cells, putative vesicular bodies were observed in association with the cell wall (Figure 1A-C), providing additional evidence for the existence of an extracellular vesicular transport mechanism. To address whether vesicles could be observed during infection by encapsulated cryptococci, the presence of vesicles in vivo was evaluated by electron microscopy of C57BL/6 mice infected intratracheally with *C. neoformans*. TEM analysis demonstrated extracellular vesicular structures near the edge of the capsule 2 h after infection (Figs. 1D), as well as hypoluscent vesicular structures in the cryptococcal cell wall (Figure 1E). Similar results were observed when mice were killed 48 h or 7 d after infection (data not shown).

These results implied that cryptococcal vesicles could pass through the cell wall to be released to the extracellular environment. Consequently, we hypothesized that these structures would be found in culture supernatants. Transmission electron microscopy of material recovered by concentration of *C. neoformans* culture supernatants followed by differential sedimentation revealed the presence of vesicular bodies (Figure 1F-H). Vesicle size and electron density varied considerably but, essentially, all of them corresponded to spherical bodies with evident bilayered membranes.

GlcCer and sterols are present in vesicular lipid extracts. Pellets obtained after centrifugation of culture supernatants at 100,000 *g* were extracted with different mixtures of organic solvents and these preparations were analyzed by HPTLC. In different vesicle preparations, bands with migration rates corresponding to the GlcCer standard were detected in lipid extracts from both acapsular and encapsulated *C. neoformans* cells (Figure 2, inset). Vesicular extracts from both encapsulated and acapsular isolates also present molecules with R_f corresponding to ergosterol, the principal fungal sterol. In order to confirm that sterols and GlcCer are in fact the molecules detected by HPTLC analysis, vesicle lipids from encapsulated cells were examined by ESI (MS and MS/MS) in positive mode. Although several molecular ions were detected (Figure 2), the analysis was focused on sterols and GlcCer, the major species detected in TLC analysis.

The principal cerebroside produced by *C. neoformans* is *N*-2'-hydroxyoctadecanoyl-1-beta-D-glucopyranosyl-9-methyl-4,8-sphingadienine, as demonstrated by our group (30). The full spectra (scanned from 300-800 *m/z*) of neutral lipids obtained after Folch's partition in fact suggested the presence of GlcCer with Li^+ adducts. Monolithiated peaks at *m/z* 734 $[M+Li^+]^+$ and 762 $[M+Li^+]^+$ were observed and revealed a profile similar to what has been described by our group and others for fungal GlcCer (1, 24, 30). These molecular ions correspond to *N*-2'-hydroxyhexadecanoyl- and *N*-2'-hydroxyoctadecanoyl-1-beta-D-glucopyranosyl-9-methyl-4,8-sphingadienine, as confirmed after ESI-MS/MS analysis (Figs. 2B and 2C). Loss of water $[M-H_2O+Li^+]^+$ generated peaks at *m/z* 716 and 744. Abundant lithiated aglycon $[M\text{-hexose}+Li^+]^+$ peaks with *m/z* at 572 and 600 corresponded, respectively, to loss of 162 units from the molecular ions at *m/z* 734 and 762. The variation of 28 units among these peaks indicates the presence of two species of hydroxylated fatty acids, containing 16 or 18 carbons. The presence

of an abundant ion peak at *m/z* 480 in both spectra, corresponding to loss of OH C_{16} and OH C_{18} fatty acids $[M\text{-}FA+Li^+]^+$, confirmed this structural diversity.

Ergosterol and obtusifoliol are the major sterols produced by *C. neoformans* (18). The major peaks at *m/z* 397 and 435 (Figure 2) supported, respectively, the occurrence of a $[M+H^+]^+$ ion corresponding to ergosterol and a $[M+Li^+]^+$ peak compatible with a molecule differing from obtusifoliol in 2 units of mass. For structural elucidation, these ions were submitted to ESI-MS/MS scan (Figs. 2D and E). The molecular ion at *m/z* 397 $[M+H]^+$ gave rise to fragments at *m/z* 285 ($[C_{20}H_{29}O]^+$, 302 ($[C_{22}H_{38}]^+$), 190 ($[C_{14}H_{22}]^+$), 173 ($[C_{13}H_{17}]^+$) and 154 ($[C_{11}H_{22}]^+$) compatible with the sterol profile of fragmentation proposed by Scallen, et al. (33), and with a commercial standard of ergosterol (data not shown). The fragmentation of the molecular ion at *m/z* 435 $[M+Li]^+$, yielded daughter ions at *m/z* 417 $[M\text{-}H_2O+Li^+]^+$, 407 ($[C_{28}H_{48}OLi]^+$), 267 ($[C_{29}H_{32}Li]^+$) and 186 ($[C_{13}H_{24}Li]^+$). Minor ions at *m/z* 391, 351, 337, 311, 295, 284 and 199 were also observed. All of these peaks were compatible with a monolithiated molecular ion corresponding to an obtusifoliol-like molecule lacking the double bond between carbons 8 and 9. This structure was therefore identified as 4,14-dimethylergosta-24(24^1)-en-3β-ol.

Vesicle production requires viable *C. neoformans* cells. After growth for 72 h, the viability of the cryptococcal population was very close to 100%, as determined by PI staining (data not shown). However, even with high indices of viability, the possibility that the vesicles originated from a minor fraction of dead cells could not be discarded. In this context, we first evaluated the ability of *C. neoformans* to use radioactive precursors of ceramide to produce [^{3}H]ceramide-containing vesicles, based on the evidence that GlcCer is present in vesicle extracts. The detection of [^{3}H]GlcCer in vesicle fractions from strain 24067 (Figure 3A) suggested that *C.*

neoformans metabolically incorporated the radioactive precursors and secreted their corresponding products in vesicular preparations. The insignificant levels of [^{3}H]GlcCer detection in sterile media containing the radioactive precursors and in 100,000 *g* supernatants supported this hypothesis. In addition, GlcCer-containing vesicles being transferred from the plasma membrane to the cell wall were detected by immunogold labeling with antibodies to GlcCer followed by analysis by TEM (Figure 3B). Wall-associated extracellular vesicular bodies were also observed in these preparations.

The possibility that the vesicles could be the products of dead cells was also considered, given that lipids are present in the membranes of all organelles. Thus, we compared lipid profiles obtained in regular vesicle fractions with those obtained from dead cells. To avoid false negative results, several methods of fungal killing were evaluated, including metabolic inhibition (sodium azide treatment) and protein denaturation (mild heat exposure). *C. neoformans* was grown under the conditions used for vesicle production, and then the supernatant was collected and used for vesicle purification. Cell viability decreased by 83 and 99 %, respectively, after treatment with azide or heat (Figure 3C). The treated yeast cells were removed as described in Experimental Procedures and the supernatants centrifuged at 100,000 *g*. GlcCer was detected in 100,000 *g* fractions from living, but not heat- or azide-treated cells, as determined by HPTLC using a purified standard of ceramide monohexoside. Sterol analysis revealed that compounds with migration rates corresponding to an ergosterol standard were detected in 100,000 *g* fractions from supernatants of living and azide-treated cells, but not in preparations from heat-killed cryptococci. We speculate that the detection of sterols in vesicles from azide-treated cells could be the result of stress-associated secretory activity during metabolic inhibition. Also, the sterol content of 100,000 *g* fractions from living and azide-treated cells was analyzed by densitometry,

showing that the detection of sterol in the former was 2.5 fold higher (data not shown). In summary, these results suggest that the vesicles described here are produced and excreted by living *C. neoformans*, rather than released from dead cells. Results using the different strains currently studied were very similar.

GXM is contained inside cryptococcal vesicles. The presence of GXM in vesicular bodies was evaluated by immunogold labeling of purified vesicles with mAb 18B7 followed by TEM analysis (Figure 4A). Antibody binding to purified vesicles was largely concentrated in the vesicular matrix. The presence of GXM was confirmed by the fact that the antibody reacted strongly with their contents (obtained by solvent-mediated lysis) in ELISA tests (Figure 4B). As an additional control, the supernatant obtained before vesicle lysis was also assayed, and the content of GXM in this preparation was around 10-fold lower than the amount of GXM in the vesicle pellet. The most straightforward interpretation of these results is that GXM is contained primarily in the intravesicular compartment, but that some material is found in solution, probably as a result of vesicle damage and/or disruption in handling. To confirm the premise that GXM was intravesicular, we removed the extracellular GXM by sequential passage of the vesicle preparation over a column of Sepharose-bound mAb 18B7 (Figure 4C). In this experiment, the vesicle fraction and a vesicle-depleted supernatant were consecutively passed through the antibody-containing resin. While the GXM content in the supernatant seemed to decrease after each step of incubation with the resin, it stabilized when the vesicle preparation was used. Hence, we conclude that the vesicles contain GXM.

To exclude the possibility that GXM-containing vesicles were formed extracellularly by random incorporation of the polysaccharide into liposomes instead of being secreted, the

minimal medium was supplemented with GXM and inoculated with Cap67 cells. After 72 h of growth at 30°C, Cap67 supernatants were collected for vesicle purification. Alternatively, acapsular cells were grown in the absence of GXM, and the polysaccharide was added to culture supernatants after removal of yeast cells. Vesicle purification in these systems followed by polysaccharide determination demonstrated the absence of significant amounts of GXM in the 100,000 *g* fractions (Figure 4D), suggesting that the association of GXM and vesicles was not a simple artifact of polysaccharide incorporation into liposomes or polysaccharide-facilitated formation of lipid vesicles. Interestingly, no significant loss of GXM in supernatants was observed when the polysaccharide was added to the culture after fungal growth. When the medium was supplemented with GXM before inoculation of acapsular cells, however, only one third of the total amount of the polysaccharide initially added was detected in supernatants. This result could be linked to the well known ability of Cap67 cells to incorporate GXM into its cell wall. In fact, immunofluorescence analysis with mAb 18B7 revealed that, after growth in the presence of GXM, the surface of Cap67 cells were stained by the antibody to polysaccharide (data not shown).

GXM content in vesicles correlates with capsule synthesis. If GXM was packaged inside vesicles for extracellular transport we hypothesized that the conditions that promoted capsule growth would also be associated with an increase in supernatant vesicles. To evaluate the possible correlation between capsule synthesis and vesicle secretion, cryptococci were stimulated to produce capsule, and supernatants were evaluated for vesicle content. Vesicles were obtained by ultracentrifugation at 100,000 *g* and pellets were resuspended in TBS for GXM analysis by capture ELISA. GXM concentrations in 100,000 *g* fractions in the different conditions of capsule

induction were normalized to the number of cells in the culture after each condition of stimulation. In parallel, yeast cells were collected by centrifugation, washed in PBS and fixed in 2% paraformaldehyde for microscopic observation after India ink staining. After 24h of incubation of cryptococci in diluted Sabouraud broth, capsule expression was approximately two-fold higher than that in cells incubated for 6h (Figure 5A). Similarly, the content of GXM in the vesicle fraction after 24 h was two-fold higher than that observed after incubation of cryptococci during 6h (Figure 5B).

Incorporation of vesicular GXM into the surface of acapsular cryptococci. The correlation between capsule growth and GXM content in the vesicle fraction suggested that *C. neoformans* must have mechanisms to extract the polysaccharide from vesicles. To evaluate this hypothesis, acapsular *C. neoformans* cells were incubated in the presence of purified vesicles and then evaluated by immunofluorescence with mAb 18B7. A strong fluorescent reaction of the antibody with acapsular cells was observed after incubation with the vesicle suspension (Figure 6), suggesting that *C. neoformans* can release GXM from vesicular bodies and uses it for capsule growth. Control yeasts, which had not been incubated with mAb 18B7 or vesicle preparations, presented very weak levels of fluorescence. Yeast cells incubated with non-vesicular purified GXM also became encapsulated (data not shown), as extensively described in previous studies.

Detection of GXM-containing vesicles from regular cultures or infected macrophages after sucrose gradient separation. Given the size diversity of the vesicles demonstrated in Figure 1, a more detailed analysis of vesicle production by *C. neoformans* during its regular growth was performed by using ultracentrifugation followed by flotation on a step sucrose gradient (15).

After ultracentrifugation for 18h, twelve fractions were obtained. HPLC analysis revealed the presence of peaks with retention times similar to that of a standard GlcCer in all fractions (Figure 7A). The area of each peak varied depending on the sucrose concentration in each fraction. Analysis of the presence of GXM in sucrose gradient fractions was performed using the capture ELISA test. The results shown in Figure 7B indicate that the maximum indices of polysaccharide detection were measured in the most concentrated sucrose fractions, suggesting that packaging of GXM into lipid membranes results in highly dense vesicles. The influence of experimental conditions on GXM distribution in gradient fractions was analyzed by changing sucrose concentrations. Using different conditions, the highest content of GXM was always found in the most concentrated sucrose fractions (data not shown).

Based on the property that macrophages (J774.16 cells) infected with *C. neoformans* become lysed after prolonged periods of incubation (38), supernatants of yeast-infected macrophage cells were collected for vesicle purification. After separation of these fluids by ultracentrifugation associated with sucrose gradient, the presence of GXM was analyzed in each fraction. Comparing the profile obtained of infection-derived vesicles with that observed in regular cultures (Figure 7B), two additional regions containing high levels of polysaccharide were observed in preparations obtained from infected macrophages. These results support the idea that *C. neoformans* produces GXM-containing vesicles inside host cells or, alternatively, induces the production of host-derived membrane domains filled with the polysaccharide, as previously suggested (38).

Discussion

Secretion of macromolecules (molecular weight > 1 million) by fungal cells is a puzzling topic. To reach the extracellular environment, secreted molecules must cross the cell wall molecular network, a porous but very rigid complex. In *C. neoformans*, it has been recently demonstrated that GXM is trafficked within cytoplasmic secretory vesicles (40), supporting a model that capsular materials are synthesized in the Golgi and targeted to the plasma membrane for exocytosis. However, it remains unknown how the vesicles would reach the extracellular environment to be used for capsule expression. In this regard, we present evidence that the major virulence factor of *C. neoformans* is secreted by a novel mechanism involving the release of membrane vesicles through the cell wall. Vesicle secretion is apparently not exclusively related to GXM traffic, since lipid-containing extracellular vesicles were observe in acapsular cells.

The possibility that the cell wall of *C. neoformans* is permeable to the passage of intact vesicular structures was supported by microscopic analysis of acapsular cells cultivated in vitro and encapsulated cells from infected mice. Putative vesicular bodies in association with the cell wall and in the extracellular milieu were observed in both acapsular and encapsulated cells, suggesting that *C. neoformans* can use vesicular transport to secrete different compounds. Microscopic analysis of pellets obtained after differential centrifugation of culture supernatants revealed intact vesicles ranging in size from 60-300 nm. Despite this heterogeneity, the vesicles had the common appearance of being rounded and defined by a lipid bilayered membrane. Differences in electron density were observed, suggesting heterogeneity in vesicular contents. The size of the vesicles was consistent with those shown in Figure 1 and with the size predicted from the early electron microscopic studies that showed intracellular GXM in what appeared to

be vesicular structures (11, 14, 40). In those studies, the vesicular structures were 100 to 300 nm in diameter, which is within the range of the vesicles described here.

Glycosphingolipids, sterols and GPI-anchored proteins form detergent-insoluble lipid rafts on the plasma membrane (23). They are required for the processing of surface proteins in yeasts, making part of vesicles that link the RES to Golgi to the plasma membrane (34). In *C. neoformans*, it has been suggested that GlcCer-containing vesicles migrate from the cell membrane to the cell wall (1, 25, 30). In the present study, lipid analysis by mass spectrometry revealed that a glycosphingolipid (GlcCer) and sterol are components of extracellular vesicles, supporting the idea that they are enriched in lipid rafts. The physiologic production of GlcCer as vesicle components was strengthened by the observation that [^{3}H]glucosylceramide was metabolically incorporated in vesicular fractions. Lipids were not detected in supernatants from dead cells, strongly suggesting that *C. neoformans* physiologically secretes vesicles. The visualization of GlcCer-containing vesicle-like structures in both cell wall and extracellular spaces of *C. neoformans* cells supports the view that these structures are active products of fungal cells. The relevance of these findings to the pathogenesis and control of cryptococcosis is supported by different studies, which demonstrated that GlcCer induces the production of antimicrobial antibodies during human infection (30) and is the target of defensins from insect and plant cells (35). More recently, it has been demonstrated that GlcCer expression regulates cryptococcal virulence and is essential for fungal growth in neutral/alkaline pH *in vitro* and *in vivo* (28).

Sterol derivatives, including ergosterol and an obtusifoliol-like molecule, were also characterized as lipid components of vesicle membranes. Ergosterol and obtusifoliol have been previously described as major sterol components of *C. neoformans* (18) but, to our knowledge,

this is the first demonstration of 4,14-dimethylergosta-24(24[1])-en-3β-ol in cryptococcal membranes. The presence of other classes of hydrophobic compounds is evidently expected and, indeed, additional molecular ions were observed in ESI-MS analysis. The lack of detection of these molecules by HPTLC could be due to either low amounts of each individual lipid component or non-appropriated conditions of separation and staining. The fact that other lipids are clearly relevant to physiology and pathogenesis of *C. neoformans* (16, 17, 21) justifies the characterization of other components of vesicle membranes.

GXM, the principal capsular polysaccharide of *C. neoformans*, was detected in vesicle preparations by serological approaches. The possibility that polysaccharide aggregates were contaminating 100,000 g fractions was discarded, since vesicle preparations were purified in a mAb 18B7-bound resin. A definitive association between GXM and vesicles was obtained by immunogold labeling of the vesicles with an anti-GXM antibody followed by TEM analysis, which revealed that the polysaccharide is indeed surrounded by extracellular membrane domains. This information was supported by the fact that vesicle formation was not an artifact of polysaccharide-mediated effects on lipids (Figure 4D) and that the polysaccharide and GlcCer, a lipid marker of cryptococcal vesicles, were concomitantly detected in fractions from a sucrose gradient. In this analysis, the polysaccharide content is directly related to vesicular density, which is in agreement with the high viscosity described for GXM (22).

McFadden and co-workers have recently provided experimental evidence suggesting that capsule growth involves the production of GXM fibers that are released from, rather than attached to the cell (22). In this model, capsule construction would depend on the self-association of GXM fibers, in which newly synthesized molecules would be secreted into the extracellular environment and further incorporated throughout the capsule by becoming entangled in existing

capsular material. A new model of capsule growth was recently proposed whereby the capsule grows by apical extension (41). Vesicular transport to the capsular edge followed by polysaccharide unloading and polysaccharide self-assembly into a capsule would provide a potential mechanism for apical growth. Such a mechanism may have an inherent error rate such that some vesicles could be released to the extracellular space without unloading and accumulate in the culture supernatant. Alternatively, material destined for capsule or extracellular secretion may be found in different vesicular fractions such that vesicles recovered represent deliberate extra-capsular polysaccharide transport. We, therefore, hypothesized that *C. neoformans* could release capsular polysaccharides inside vesicles, which would be further lysed by still unknown mechanisms. The fact that the detection of GXM in 100,000 *g* fractions is higher when capsule expression is more efficient in *C. neoformans* supports this idea. The observation that acapsular mutants can bind GXM from purified vesicles indicate that *C. neoformans* is indeed able to lyse vesicles and use its internal content, possibly through the activity of exocellular lipases (5).

Our current results and previous reports (11, 14, 40) indicate that vesicles are synthesized intracellularly and transferred to the cell surface, from where they are secreted to the extracellular environment. It remains unknown how vesicles with an average diameter of 160 nm cross the fungal cell wall, a highly complex and dynamic structure (25). One possible explanation comes from the observation that the cell wall of *Saccharomyces cerevisiae* presents regular pores of around 200 nm, which can be increased to 400 nm under stress conditions (7). Therefore, despite being a rigid and complex structure, the fungal cell wall could allow the passive passage of particles in the range of 60 to 300 nm, dimensions that could accommodate the vesicles described here. Another mechanism for extracellular transport could involve motor proteins. In *Aspergillus fumigatus*, a 180-kDa polypeptide recognized by anti-myosin antibodies

was found to be concentrated in cell wall and plasma membrane fractions of conidia (9). Immunoelectron microscopy with an anti-myosin antiserum revealed that the antigen is mainly distributed under the plasma membrane region, although it is also clearly detected in different layers of the cell wall. The characterization of cell wall motor proteins in fungal cells will possibly contribute to the understanding of how vesicles are transported to the extracellular milieu. Our current conclusions from electron microscopy analyses of acapsular and encapsulated *C. neoformans* point to the presence of vesicles in different compartments of the cell surface, including the capsule network of 24067 cells.

The immunological activity of GXM (for review, 39) and lipids (1, 24, 25, 30) has been demonstrated in different studies. Consequently, delivery of GXM in vesicles to target host tissues could involve a twin payload of immunomodulating molecules that can interfere with immune function. Our current results and previous reports suggest that *C. neoformans* secretes capsular components during the infection of different host cells. In macrophages infected by cryptococci, GXM is released by ingested yeast cells, followed by damage to the phagosomal membrane and cytoplasmic accumulation of polysaccharide-containing vesicles (38). In the current study, the distribution of GXM in fractions obtained from ultracentrifugation associated with a sucrose gradient markedly differed when culture fluids of *C. neoformans* and supernatants from infected macrophages were compared. When macrophage-derived supernatants were analyzed, an additional peak of polysaccharide detection was observed, which could be explained by production of vesicles of different natures during the interaction of *C. neoformans* these cells, as previously suggested by Tucker and Casadevall (38). The currently presented data also indicates that *C. neoformans* produces extracellular vesicles *in vivo*, supporting the idea that vesicular transport is relevant for polysaccharide release during infection. This result may have

an impact on the understanding of the immunomodulatory activity of GXM, since its secretion during infection is accompanied by release of other immunologically active molecules, such as GlcCer and other still uncharacterized molecules.

In summary, we report the existence of membrane vesicles containing capsular polysaccharide in *C. neoformans* cultures and host cells infected with this pathogen. In contrast to prokaryotes, *C. neoformans* capsular polysaccharide is synthesized in the cell body and transported extracellularly for capsule assembly by a mechanism that involves the production of vesicles. Hence, our results and other reports (11, 14, 31, 32, 40) suggest that the eukaryotic solution to the problem of capsular assembly takes advantage of a sophisticated trans-cell wall vesicular transport secretory mechanism that is not available in prokaryotes. The discovery that polysaccharide is packaged in vesicles containing immunologically active lipids has the potential to revolutionize our views of capsule assembly, extracellular polysaccharide shedding and the mechanisms by which GXM mediates immunosuppression.

Acknowledgments

MLR was the recipient of an International Fellowship for Latin America, provided by the American Society for Microbiology, and is supported by grants from Conselho Nacional de Desenvolvimento Científico e Tecnológico (CNPq-Brazil), Fundação Universitária José Bonifácio (FUJB-Brazil) and Fundação de Amparo a Pesquisa do Estado do Rio de Janeiro (FAPERJ-Brazil) and Programa de Nanociência e Nanotecnologia, MCT-CNPq (to KM). LN is supported by CNPq-Brazil. AC is supported by NIH grants AI033142, AI033774, AI052733, and HL059842. We thank Eliandro Lima, Yvonne Kress and the Albert Einstein College of Medicine Analytical Imaging Facility staff for help with the electron microscopy. We also thank Igor C. Almeida and Sirlei Daffre for support with mass spectrometry analysis. We are indebted to Jorge José Bastos Ferreira for helpful discussions.

References

1. **Barreto-Bergter, E., M. R. Pinto, and M. L. Rodrigues.** 2004. Structure and biological functions of fungal cerebrosides. An. Acad. Bras. Cienc. **76:**67-84.
2. **Casadevall, A., J. Mukherjee, and M. D. Scharff.** 1992. Monoclonal antibody based ELISAs for cryptococcal polysaccharide. J. Immunol. Methods **154:**27-35.
3. **Casadevall, A., W. Cleare, M. Feldmesser, A. Glatman-Freedman, D. L. Goldman, T. R. Kozel, N. Lendvai, J. Mukherjee, L. A. Pirofski, J. Rivera, A. L. Rosas, M. D. Scharff, P. Valadon, K. Westin, and Z. Zhong.** 1998. Characterization of a murine monoclonal antibody to *Cryptococcus neoformans* polysaccharide that is a candidate for human therapeutic studies. Antimicrob. Agents Chemother. **42:**1437-1446.
4. **Chang, Y. C., and K. J. Kwon-Chung.** 1994. Complementation of a capsule-deficient mutation of *Cryptococcus neoformans* restores its virulence. Mol. Cell. Biol. **14:**4912-4919.
5. **Chen, S. C., L. C. Wright, R. T. Santangelo, M. Muller, V. R. Moran, P. W. Kuchel, and T. C. Sorrell.** 1997. Identification of extracellular phospholipase B, lysophospholipase, and acyltransferase produced by *Cryptococcus neoformans*. Infect. Immun. **65:**405-411.
6. **Cherniak, R., L. C. Morris, B. C. Anderson, and S. A. Meyer.** 1991. Facilitated isolation, purification, and analysis of glucuronoxylomannan of *Cryptococcus neoformans*. Infect. Immun. **59:**59-64.

7. **De Souza Pereira, R., and J. Geibel.** 1999. Direct observation of oxidative stress on the cell wall of Saccharomyces cerevisiae strains with atomic force microscopy. Mol. Cell. Biochem. **201:**17-24.

8. **Dromer, F., J. Salamero, A. Contrepois, C. Carbon, and P. Yeni.** 1987. Production, characterization, and antibody specificity of a mouse monoclonal antibody reactive with *Cryptococcus neoformans* capsular polysaccharide. Infect. Immun. **55:**742-748.

9. **Esnault, K., B. el Moudni, J. P. Bouchara, D. Chabasse, and G. Tronchin.** 1999. Association of a myosin immunoanalogue with cell envelopes of *Aspergillus fumigatus* conidia and its participation in swelling and germination. Infect. Immun. **67:**1238-1244.

10. **Feldmesser, M., A. Casadevall, Y. Kress, G. Spira, and A. Orlofsky.** 1997. Eosinophil-*Cryptococcus neoformans* interactions in vivo and in vitro. Infect. Immun. **65:**1899-1907.

11. **Feldmesser, M., Y. Kress, and A. Casadevall.** 2001. Dynamic changes in the morphology of *Cryptococcus neoformans* during murine pulmonary infection. Microbiology **147:**2355-2365.

12. **Feldmesser, M., Y. Kress, P. Novikoff, and A. Casadevall.** 2000. *Cryptococcus neoformans* is a facultative intracellular pathogen in murine pulmonary infection. Infect. Immun. **68:**4225-4237.

13. **Folch, J., M. Lees, and G. H. Sloane Stanley.** 1957. A simple method for the isolation and purification of total lipids from animal tissues. J. Biol. Chem. **226:**497-509.

14. **Garcia-Rivera, J., Y. C. Chang, K. J. Kwon-Chung, and A. Casadevall.** 2004. *Cryptococcus neoformans* CAP59 (or Cap59p) is involved in the extracellular trafficking of capsular glucuronoxylomannan. Eukaryot. Cell. **3:**385-392.

15. **Gutwein, P., S. Mechtersheimer, S. Riedle, A. Stoeck, D. Gast, S. Joumaa, H. Zentgraf, M. Fogel, and D. P. Altevogt.** 2003. ADAM10-mediated cleavage of L1 adhesion molecule at the cell surface and in released membrane vesicles. FASEB J. **17:**292-294.

16. **Heung, L. J., A. E. Kaiser, C. Luberto, and M. Del Poeta.** 2005. The role and mechanism of diacylglycerol-protein kinase C1 signaling in melanogenesis by *Cryptococcus neoformans*. J. Biol. Chem. **280:**28547-28555.

17. **Heung, L. J., C. Luberto, A. Plowden, Y. A. Hannun, and M. Del Poeta.** 2004. The sphingolipid pathway regulates Pkc1 through the formation of diacylglycerol in *Cryptococcus neoformans*. J. Biol. Chem. **279:**21144-21153.

18. **Ibrahim, A.S., H. Sanati, and M. A. Ghannoum**. 1996. Lipids of *Cryptococcus neoformans*. In Lipids of pathogenic fungi, R. Prasad and M. A. Ghannoum, ed. (Boca Raton, USA: CRC Press), pp. 156-167.

19. **Kozel, T. R.** 1995. Virulence factors of *Cryptococcus neoformans*. Trends Microbiol. **3:**295-299.

20. **Larsen, R. A., P. G. Pappas, J. Perfect, J. A. Aberg, A. Casadevall, G. A. Cloud, R. James, S. Filler, and W. E. Dismukes.** 2005. Phase I evaluation of the safety and

pharmacokinetics of murine-derived anticryptococcal antibody 18B7 in subjects with treated cryptococcal meningitis. Antimicrob. Agents Chemother. **49:**952-958.

21. **Mare, L., R. Iatta, M. T. Montagna, C. Luberto, and M. Del Poeta.** 2005. APP1 transcription is regulated by inositol-phosphorylceramide synthase 1-diacylglycerol pathway and is controlled by ATF2 transcription factor in *Cryptococcus neoformans*. J. Biol. Chem. **280:**36055-36064.
22. **McFadden, D. C., M. De Jesus, and A. Casadevall.** 2006. The physical properties of the capsular polysaccharides from *Cryptococcus neoformans* suggest features for capsule construction. J. Biol. Chem. **281:**1868-1875.
23. **Muniz, M., and H. Riezman**. 2000. Intracellular transport of GPI-anchored proteins. EMBO J. **19**:10-15.
24. **Nimrichter, L., M. D. Cerqueira, E. A. Leitao, K. Miranda, E. S. Nakayasu, S. R. Almeida, I. C. Almeida, C. S. Alviano, E. Barreto-Bergter, and M. L. Rodrigues.** 2005. Structure, cellular distribution, antigenicity, and biological functions of Fonsecaea pedrosoi ceramide monohexosides. Infect. Immun. **73:**7860-7868.
25. **Nimrichter, L., M. L. Rodrigues, E. G. Rodrigues, and L. R. Travassos.** 2005. The multitude of targets for the immune system and drug therapy in the fungal cell wall. Microbes Infect. **7:**789-798.
26. **Novikoff, A. B., and P. M. Novikoff.** 1977. Cytochemical contributions to differentiating GERL from the Golgi apparatus. Histochem. J. **9**:525-551.

27. **Oscarson, S., M. Alpe, P. Svahnberg, A. Nakouzi, and A. Casadevall.** 2005. Synthesis and immunological studies of glycoconjugates of *Cryptococcus neoformans* capsular glucuronoxylomannan oligosaccharide structures. Vaccine **23:**3961-3972.

28. **Rittershaus, P. C., T. B. Kechichian, J. C. Allegood, A. H. Merrill Jr, M. Hennig, C. Luberto, and M. Del Poeta.** 2006. Glucosylceramide synthase is an essential regulator of pathogenicity of *Cryptococcus neoformans*. J. Clin. Invest. **116:**1651-1659.

29. **Rodrigues, M. L., C. S. Alviano, and L. R. Travassos.** 1999. Pathogenicity of *Cryptococcus neoformans*: virulence factors and immunological mechanisms. Microbes Infect. **1:**293-301.

30. **Rodrigues, M. L., L. R. Travassos, K. R. Miranda, A. J. Franzen, S. Rozental, W. de Souza, C. S. Alviano, and E. Barreto-Bergter.** 2000. Human antibodies against a purified glucosylceramide from *Cryptococcus neoformans* inhibit cell budding and fungal growth. Infect. Immun. **68:**7049-7060.

31. **Sakaguchi, N.** 1993. Ultrastructural study of hepatic granulomas induced by *Cryptococcus neoformans* by quick-freezing and deep-etching method. Virchows Arch. B. Cell. Pathol. Incl Mol. Pathol. **64:**57-66.

32. **Sakaguchi, N., T. Baba, M. Fukuzawa, and S. Ohno.** 1993. Ultrastructural study of *Cryptococcus neoformans* by quick-freezing and deep-etching method. Mycopathologia **121:**133-141.

33. **Scallen, T. J., A. K. Dhar, and E. D. Loughran.** 1971. Isolation and characterization of C-4 methyl intermediates in cholesterol biosynthesis after treatment of rat liver in vitro with cholestan-3 beta, 5 alpha,6 beta-triol. J. Biol. Chem. **246:**3168-3174.

34. **Sutterlin, C., T. L. Doering, F. Schimmoller, S. Schroder, and H. Riezman**. 1997. Specific requirements for the ER to Golgi transport of GPI-anchored proteins in yeast. J. Cell. Sci. **110**:2703-2714.

35. **Takeo, K., I. Uesaka, K. Uehira, and M. Nishiura.** 1973. Fine structure of *Cryptococcus neoformans* grown in vitro as observed by freeze-etching. J. Bacteriol. **113:**1442-1448.

36. **Takeo, K., I. Uesaka, K. Uehira, and M. Nishiura.** 1973. Fine structure of *Cryptococcus neoformans* grown in vivo as observed by freeze-etching. J. Bacteriol. **113:**1449-1454.

37. **Thevissen, K., D. C. Warnecke, I. E. Francois, M. Leipelt, E. Heinz, C. Ott, U. Zahringer, B. P. Thomma, K. K. Ferket, and B. P. Cammue.** 2004. Defensins from insects and plants interact with fungal glucosylceramides. J. Biol. Chem. **279:**3900-3905.

38. **Tucker, S. C., and A. Casadevall.** 2002. Replication of *Cryptococcus neoformans* in macrophages is accompanied by phagosomal permeabilization and accumulation of vesicles containing polysaccharide in the cytoplasm. Proc. Natl. Acad. Sci. U. S. A. **99:**3165-3170.

39. **Vecchiarelli, A.** 2000. Immunoregulation by capsular components of *Cryptococcus neoformans*. Med. Mycol. **38:**407-417.

40. **Yoneda, A and T. L. Doering**. 2006. A eukaryotic capsular polysaccharide is synthesized intracellularly and secreted via exocytosis. Mol. Biol. Cell. 2006 Oct 4, Epub ahead of print.

41. **Zaragoza, O., A. Telzak, R. A. Bryan, E. Dadachova, and A. Casadevall.** 2006. The polysaccharide capsule of the pathogenic fungus *Cryptococcus neoformans* enlarges by distal growth and is rearranged during budding. Mol. Microbiol. **59:**67-83.

42. **Zaragoza, O., and A. Casadevall.** 2004. Experimental modulation of capsule size in *Cryptococcus neoformans*. Biol. Proced. Online **6:**10-15.

Figures.

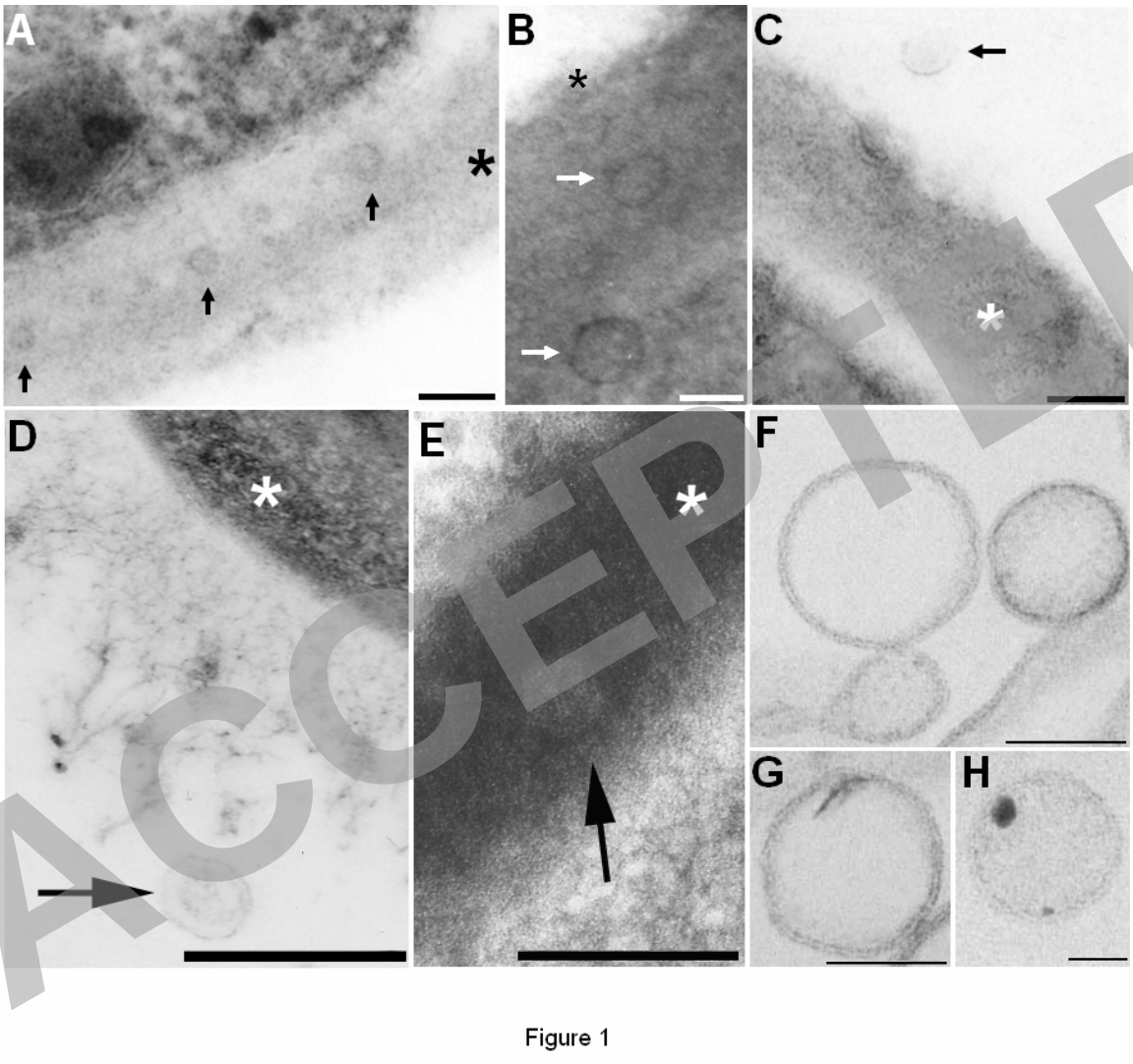

Figure 1

Figure 1. TEM of vesicles in acapsular (A-C) and encapsulated (D-H) *C. neoformans*. The occurrence of vesicles in association with the cell wall of acapsular cryptococci (A, B) or in the extracellular environment (C) is evident after in vitro growth. Vesicle-like structures were also observed in the lung following murine pulmonary infection (D-E). Putative vesicles near the edge of the capsule (D) or in the cryptococcal cell wall (E) were observed 2 h after infection. Scale bars represent 100 nm in A-C and 500 nm in D-E. Arrows point to vesicles, asterisks are on the cryptococcal cell wall. Pellets obtained by ultracentrifugation were isolated by differential

centrifugation, purified from GXM by affinity chromatography and analyzed by TEM (F-H). Extracellular vesicles with bilayered membranes and different profiles of electron density were observed. Scale bars correspond to 100 nm in F-G and 50 nm in H.

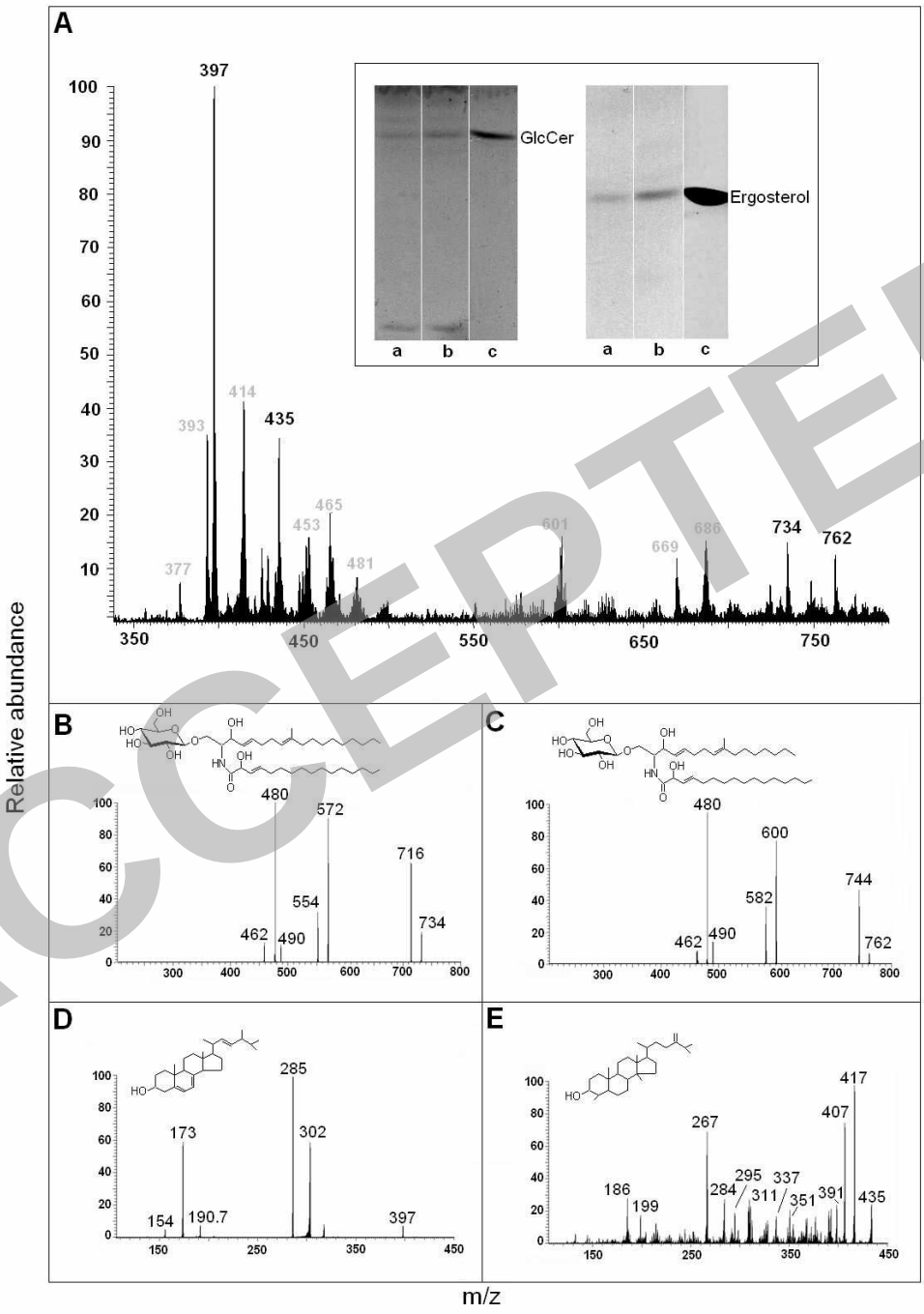

Figure 2

Figure 2. Lipid analysis of *C. neoformans* vesicles. Lipid extracts were prepared as described in Methods and analyzed by ESI-MS and HPTLC (A). Vesicle lipids with migration rates corresponding to GlcCer and ergosterol standards (c) were detected by HPTLC (inset) in preparations from both encapsulated (a) and acapsular (b) *C. neoformans*. ESI-MS analysis

demonstrated the presence of molecular ions corresponding to GlcCer (734 and 762) and sterols (435 and 397), besides other still unidentified molecules (*m/z* values in gray). Fragmentation analysis of molecular ions at *m/z* 734 (B) and 762 (C) revealed ionized species with m/z values typical of lithiated fungal cerebrosides. Ceramide structures with C_{16}- (structure B) and C_{18}- (structure C) fatty acids were detected. Hex, hexose; FA, fatty acid. Fragmentation analysis of molecular ions at m/z 397 (D) and 435 (E) revealed the presence of ergosterol (structure D) and 4,14-dimethylergosta-24(24^1)-en-3β-ol (structure E), an obtusifoliol-like structure.

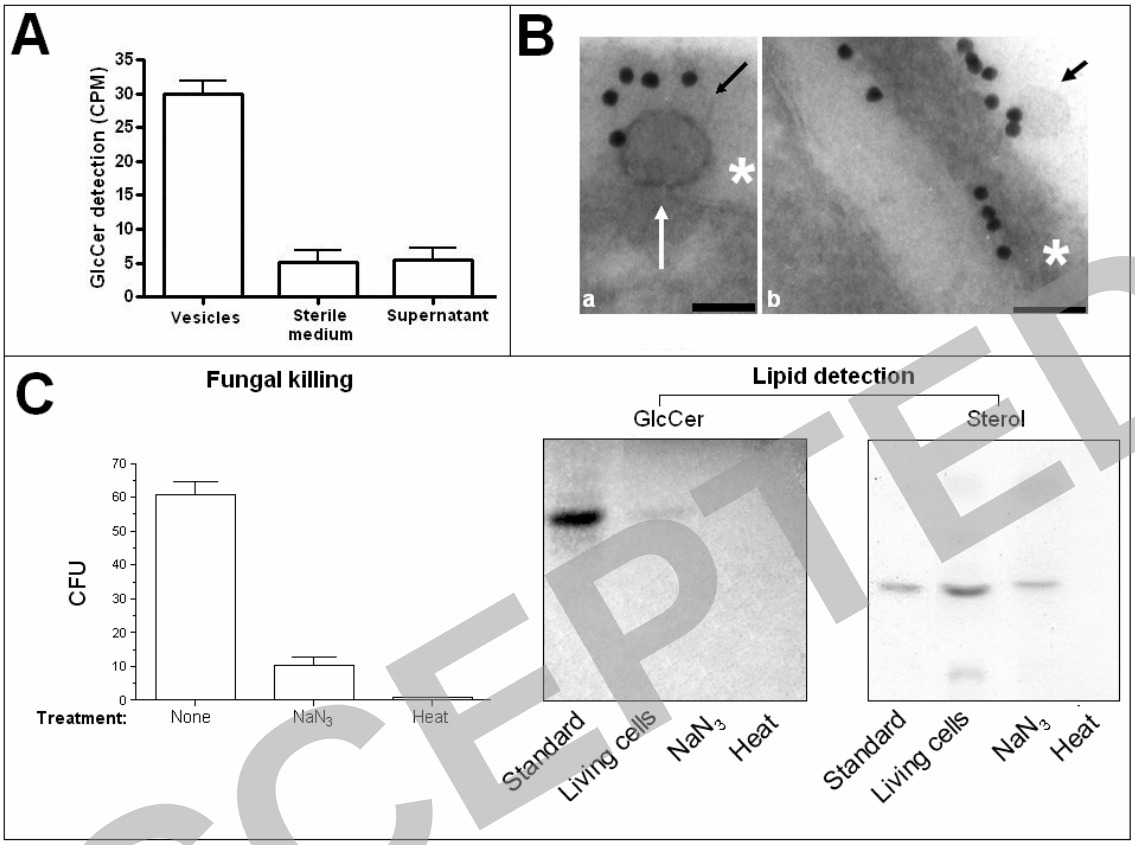

Figure 3

Figure 3. Vesicle production requires cell viability. Addition of radioactive ceramide precursors to the culture medium (A) results in the detection of significant levels of radioactive GlcCer in vesicle preparations. In 100,000 *g* pellets from sterile medium and in 100,000 *g* supernatants of grown cells, significant levels of radioactive GlcCer were not detected ($P<0.001$). B. GlcCer-containing vesicles are apparently transferred from the plasma membrane to the cell wall (a) and then secreted (b). Scale bars represent 100 nm. Arrows point to vesicles, asterisks are on the cryptococcal cell wall. C. Killing of cryptococci with sodium azide or heating demonstrates a decrease in cell viability of 83% (sodium azide) and 99% (heat), as determined by comparison with CFU counts obtained with untreated yeasts. Lipid analysis of 100,000 *g* fractions of the supernatants obtained after fungal killing revealed the detection of GlcCer in fractions from

living, but not heat- or azide-treated cells. Compounds with migration rates corresponding to an ergosterol standard were detected in 100,000 *g* fractions from supernatants of living and azide-treated cells, but not in preparations from heat-killed cryptococci.

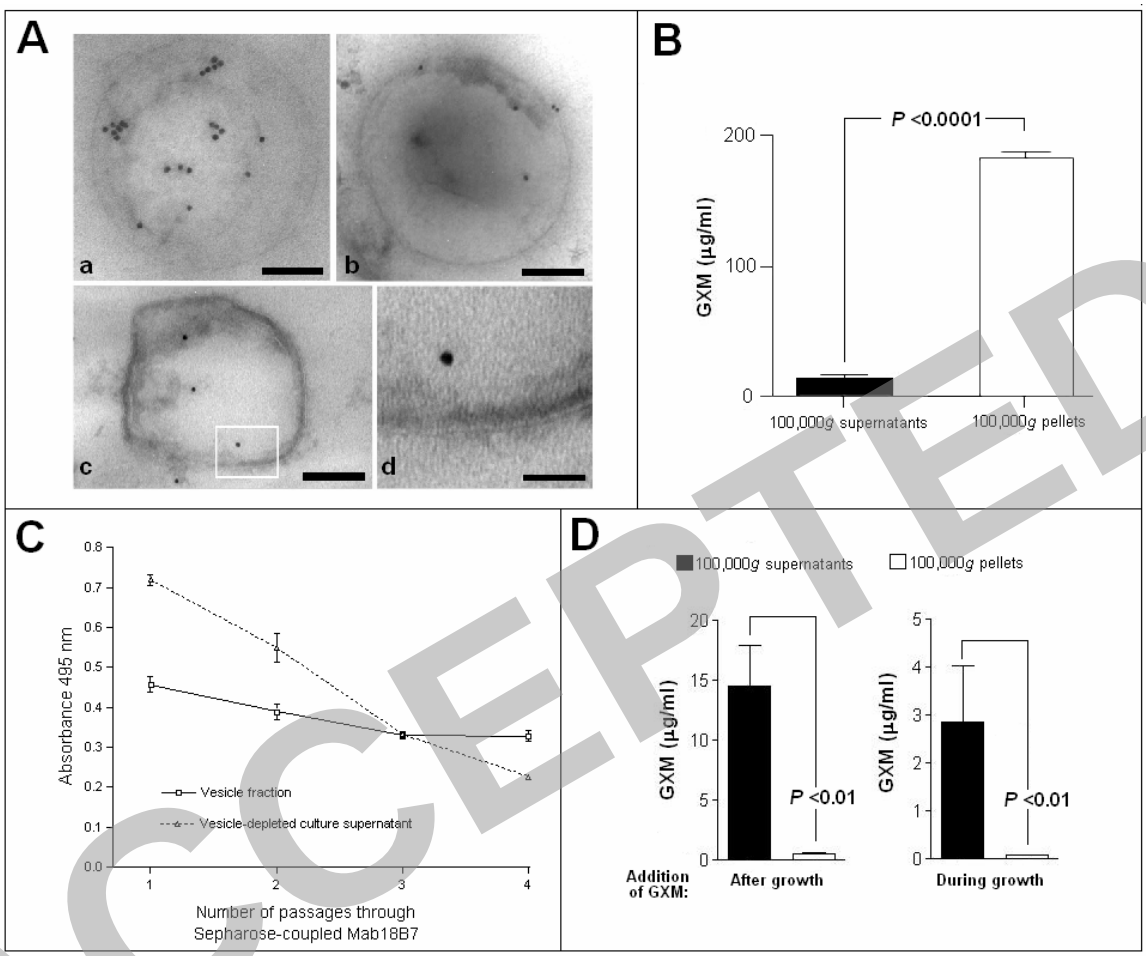

Figure 4

Figure 4. GXM is present in purified vesicles. A. Immunogold labeling of purified vesicles with mAb 18B7 revealed a preferential intravesicular distribution of GXM, as observed in different vesicular bodies (a-c). A higher magnification of the boxed area shown in c demonstrates the occurrence of bilayered membrane (d). Scale bars represent 150 (a), 180 (b), 120 (c) and 30 (d) nm. B. The presence of GXM inside the vesicles was confirmed by polysaccharide detection in purified 100,000 *g* fractions from culture supernatants (white bar). Supernatants obtained from these suspensions were assayed as a control of vesicle integrity and, in fact, GXM was detected at low levels in these preparations (black bar), suggesting that some of these structures may be disrupted. C. GXM content of vesicle suspensions and vesicle-depleted supernatants after serial

passage through a column composed of Sepharose-bound mAb 18B7. Sequential passages of vesicle-depleted supernatant through this column results in a rapid loss of reactivity while the GXM content of the vesicular preparation is relatively constant. D. GXM-containing vesicles are not formed extracellularly, since the addition of the polysaccharide to culture supernatants during or after growth of Cap67 cells is not followed by its detection in purified 100,000 *g* fractions.

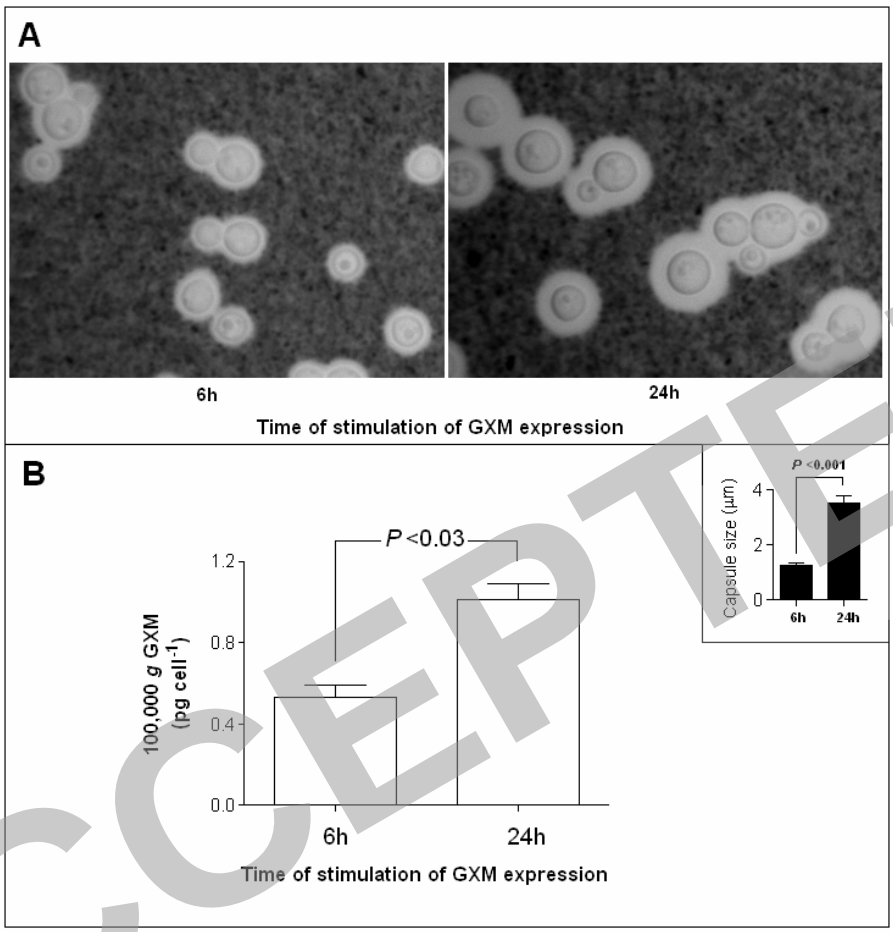

Figure 5

Figure 5. Association of capsule expression with supernatant accumulation of GXM-containing vesicles. Capsule expression was higher in yeast cells incubated for 24 h in capsule inducing media (A). The profile of GXM detection in ultracentrifugation pellets (B) was very similar to that observed for determinations of capsule size (inset), suggesting the occurrence of a correlation between capsule expression and production of vesicles containing GXM. GXM concentrations in 100,000 *g* fractions in the different conditions of capsule induction were normalized to the number of cells in the culture after each experimental condition.

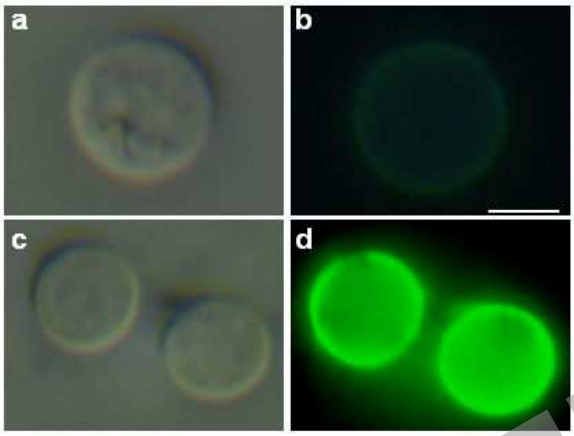

Figure 6

Figure 6. Acapsular cells of *C. neoformans* bind GXM from extracellular vesicles. Cap 67 cells were incubated for 5 h in the presence of purified vesicles and then analyzed by immunofluorescence with mAb 18B7. Control cells, not incubated with mAb 18B7, are shown in upper panels (a, b). Yeast cells that were incubated in the presence of the vesicular preparation reacted strongly with the antibody to GXM, as shown in lower panels (c, d). Left panels (a, c) represent cryptococci analyzed under differential interferential contrast, while right panels (b, d) show images in the fluorescence mode. Bar represents 2 μm.

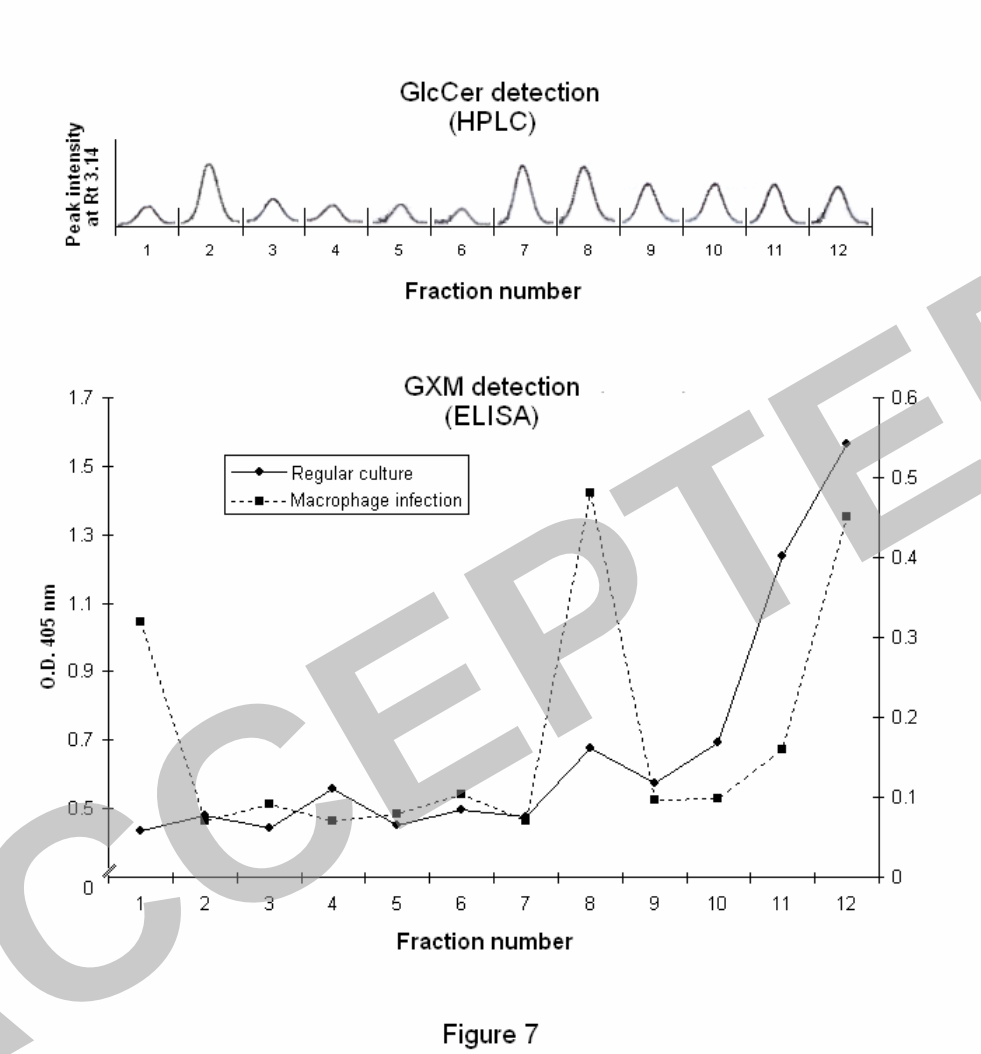

Figure 7

Figure 7. Analysis of vesicle fractions obtained after ultracentrifugation of and sucrose gradient separation. Fractions from supernatants of regular cultures were extracted with chloroform-methanol mixtures and analyzed by HPLC. In each fraction, a single peak with retention time corresponding to a GlcCer standard was detected. Analysis of the same fractions (solid line) or preparations obtained from infected macrophages (dashed line) by capture ELISA revealed different profiles of GXM distribution, although the polysaccharide was always expressively detected in the region of the gradient presenting the highest density. Lipid and polysaccharide analyses were performed at least three times, always presenting similar profiles.